Meas. Sci. Technol. **10** (1999) 269–274. Printed in the UK PII: S0957-0233(99)97963-8

Amorphous alloys as secondary standards for electron spin polarimetry

E A Seddon†, A E R Malins‡, M Petty‡§, M D Crapper‡, I R M Wardell‖¶, A K Hide‖, M Hardiman‖, Y B Xu+*, P Hucknall+, D Greig+, S Clowes# and E M McCash#

† CLRC Daresbury Laboratory, Daresbury, Warrington WA4 4AD, UK
‡ Loughborough University, Loughborough, Leicestershire LE11 3TU, UK
‖ Physics and Astronomy Division, University of Sussex, Brighton BN1 9QH, UK
+ Department of Physics and Astronomy, University of Leeds, Leeds LS2 9JT, UK
# Chemistry Department, The University of York, Heslington, York YO1 4DD, UK

Received 30 September 1998, in final form and accepted for publication 7 January 1999

Abstract. The surface magnetism of as-cast and field annealed amorphous $Co_{66}Fe_4Ni_1B_{14}Si_{15}$ in ribbon form has been studied by spin-polarized secondary electron spectroscopy, by recording energy-resolved spin asymmetry hysteresis loops and by scanning electron microscopy with polarization analysis. Large lateral variations in surface magnetization have been detected, indicating that $Co_{66}Fe_4Ni_1B_{14}Si_{15}$, in particular, and ferromagnetic melt-spun ribbons, in general, are not suitable as standard sources of polarized electrons. Deposition of an iron film onto the $Co_{66}Fe_4Ni_1B_{14}Si_{15}$ did not result in a more uniform surface but rather served to emphasize the substrate magnetic structure. Thus utilization of ferromagnetic melt-spun amorphous alloys as substrates for the growth of thin magnetic films should be undertaken with caution.

Keywords: spin polarization of photoelectrons, spin polarized secondary electron spectroscopy, spin asymmetric hysteresis, SEMPA, surface magnetism

1. Introduction

During the last 5 years the use of spin-resolving, low-energy electron spectroscopy has expanded, leading to a demand for a reliable, easy-to-use, standard source of polarized electrons for polarimeter calibration. The use of GaAs-based polarized electron sources is becoming more widespread, but they are not yet easy to use owing to the artistry required in generating a negative-electron-affinity surface and the sensitivity of this surface to contamination.

Since the overall efficiencies of polarimeters are always rather low, an attractive option is to use the relatively high polarization and intensity of the secondary electron (SE) cascade from a ferromagnet. To a first approximation, this polarization is proportional to the magnetization and hence the sample must be uniformly magnetized in order that the polarization is independent of the position across the surface used. Although the SE polarization emission spectrum has been measured accurately for single-crystalline Fe [1], the fine structure in this and the complications introduced by the use of single crystals have prompted a search for a more convenient standard.

As early as 1987, Hopster had suggested that commercially available Fe–B-based ferromagnetic amorphous metal ribbons (e.g. $Fe_{82}B_{12}Si_6$, $Fe_{60}Ni_{20}B_{20}$ and $Fe_{44}Ni_{37}B_{19}$) could be used as 'calibrated' spin-polarized electron sources [2]. These materials have many advantages; they can be conveniently mounted as closed loops which are easy to magnetize and give minimal stray fields, the isotropic SE emissions have high polarizations which vary smoothly with energy and the surface cleaning is very simple. However, these Fe-based materials have moderate-to-high magnetostriction coefficients and thus, in the as-cast (strained) state, they exhibit rich domain structures [3, 4] which are strongly influenced by any subsequently applied stresses [5, 6]. The anisotropies induced by stress can be very large and it is difficult to produce samples with a spatially uniform magnetization, even when the sample is apparently magnetically saturated. We have reported previously [7] that amorphous $Fe_{80}B_{20}$ in the as-cast state exhibits strong local variations in SE polarization which are clearly incompatible with its use as a standard. Field annealing of the Fe-based materials can improve their magnetic homogeneity [8–10], but the procedures are highly material specific and there is often a degree of recrystallization, rendering them brittle.

§ Present address: Loughborough Surface Analysis Ltd, Gas Research and Technology Centre, Ashby Road, Loughborough LE11 3WS, UK.
¶ Present address: Omicron Surface Science Ltd, Whitworth Road, Crawley RH11 7XL, UK.
* Present address: Cavendish Laboratory, Madingley Road, Cambridge CB3 0HE, UK.

More recently, Klebanoff has advocated the use of unannealed (as-cast) amorphous $Co_{66}Fe_4Ni_1B_{14}Si_{15}$ ribbon as a polarized electron standard [11]. Although the SE polarization from this material is only about a third that from the high-concentration Fe-based alloys (corresponding to the differences in saturation magnetization), the Co-based alloys close to this composition have essentially zero magnetostriction and so might be expected to be easily saturated to a uniformly magnetized state.

Another role for amorphous ribbons is as substrates for the deposition of thin magnetic films [12, 13]. In this case the strong exchange coupling between the film and the easily magnetized substrate can be used to magnetize the deposited film. We report here on the feasibility of using $Co_{66}Fe_4Ni_1B_{14}Si_{15}$ ribbon for each of the above purposes. Measurements both on the as-cast and on field-annealed material were made using spin-polarized secondary electron spectroscopy (SPSES) and SEMPA (scanning electron microscopy with polarization analysis).

2. Experimental details

Amorphous ribbon samples of $Co_{66}Fe_4Ni_1B_{14}Si_{15}$ (Allied Signal Inc) were used either as-cast or after field annealing at 0.08 T under flowing argon at temperatures of up to 350 °C for 5 min. For each type of experiment, 5 mm wide strips were cut parallel to the long (roll) axis of the ribbon and these were then formed into closed loops with the overlapping ends clamped together. The samples were arranged with the shiny (air) side outwards and they could be magnetized in the longitudinal direction of the loop by passing a current through a small coil wrapped around the strip.

The SPSES experiments were performed on Station 6.1 of the Synchrotron Radiation Source (SRS), which was designed for UHV (base pressure 2×10^{-10} Torr) photoemission work over the photon-energy range 80–180 eV. As a consequence of the baking out of the experimental chamber, all samples measured in it were subjected to a heating cycle after mounting (135 °C maximum). Emission was stimulated either with 135 eV photons or with 1.6 keV electrons, in each case at near glancing incidence (5–10°) and with incident beam diameters of about 0.5 mm. The spin polarization at normal emission was measured with a 'microMott' polarimeter mounted at the exit of a rotatable 50 mm radius hemispherical electron-energy analyser. Four data-acquisition channels allowed the simultaneous determination of two mutually perpendicular polarization components, P_{Long} and P_{Trans}, which are defined as longitudinal and transverse with respect to the long axis of the ribbon (both components are in the surface plane). The asymmetry, A, the directly measured parameter in a spin polarimeter, is related to P by $A = S_{eff}P$ and the instrument was operated with an effective Sherman function, S_{eff}, of 0.12. This equipment has been described in detail elsewhere [14]. The SPSES data were recorded either as asymmetry spectra, $A_{Long,Trans}(E_k)$, from samples in a fixed magnetic state, or as energy-resolved (asymmetry) hysteresis loops (ERHL), $A_{Long,Trans}(I)$, by using SEs with well defined kinetic energies, E_k. Before the SPSES measurements, the samples were cleaned *in situ* by argon-ion etching for a period of at least 2 h. This resulted in a minimization (to less than about 5%) of the C and O impurity levels detected by Auger spectroscopy.

The SEMPA images were obtained in a separate apparatus using a 1 nA unpolarized 5 keV primary electron beam focused to a 5 μm spot. Secondary electrons of energies up to about 60 eV were collected at near-normal emission and their longitudinal (with respect to the ribbon) polarization component measured in a 20 keV retarding field Mott detector (with $S_{eff} \simeq 0.14$ and of similar basic design to that utilized above). Data were obtained as 128 × 128 pixel $A_{Long}(x, y)$ images with a dwell time of 150 ms per pixel, as line scans, $A_{Long}(x)$, and as fixed position (spot-mode) $A_{Long}(I)$ hysteresis loops. The SEMPA apparatus is described in more detail elsewhere [15].

3. Results and discussion

The spin-integrated photoemission spectrum of the valence band and a 30 eV ERHL for $Co_{66}Fe_4Ni_1B_{14}Si_{15}$ have been reported previously [12]. We have measured the secondary electron polarization spectrum, $P(E_k)$, of this material at the SRS on a number of occasions, using either electron or photon excitation, and have consistently found the usual increase in polarization below 10 eV. However, the unexpected presence of a significant transverse asymmetry component indicated that the *mean* magnetization of the area probed was not collinear with the longitudinal axis of the ribbon. This prompted a more detailed investigation of lateral variations in spin asymmetry.

Our first studies of the uniformity of the ribbons were made by recording electron-excited ERHLs at various positions along the transverse (short) axis of a sample; typical results for the as-cast material, taken at 1 eV, are shown in figure 1. Clearly, these loops reveal considerable variations in squareness, symmetry about zero field, coercive field and, most importantly, in the asymmetry changes $\Delta A_{Long}(I)$ and $\Delta A_{Trans}(I)$. At only one position do the latter two parameters have values close to the expected ones of about ±0.017 and zero, respectively. This exercise was repeated but using 135 eV photons as the primary excitation source and selecting 0.5 eV SEs. Similar lateral variations were observed, see figure 2, indicating that the problem is unrelated to the particular excitation source used. It is also unlikely that the variations are related to the topmost surface layer since ERHLs taken at these very low E_k values are more representative of the bulk [16]. We have attempted to make magneto-optical Kerr effect (MOKE) measurements on $Co_{66}Fe_4Ni_1B_{14}Si_{15}$ ribbon in the same manner as reported for $Fe_{80}B_{20}$; however, it proved impossible to obtain hysteresis loops from this material.

In order to investigate the finer-scale spatial variation of the magnetization in the as-cast state, SEMPA data were obtained from this material. Figure 3 shows a sequence of images from the same 1.9 mm × 2.6 mm area in different magnetic states. The middle two panels are of the remanent state and show clearly that the upper portion of the imaged area of this particular (closed loop) sample is demagnetizing at zero magnetizing current. We note especially that the streak-shaped region at the very top of these images is always antiparallel to its surroundings in the remanent state. This

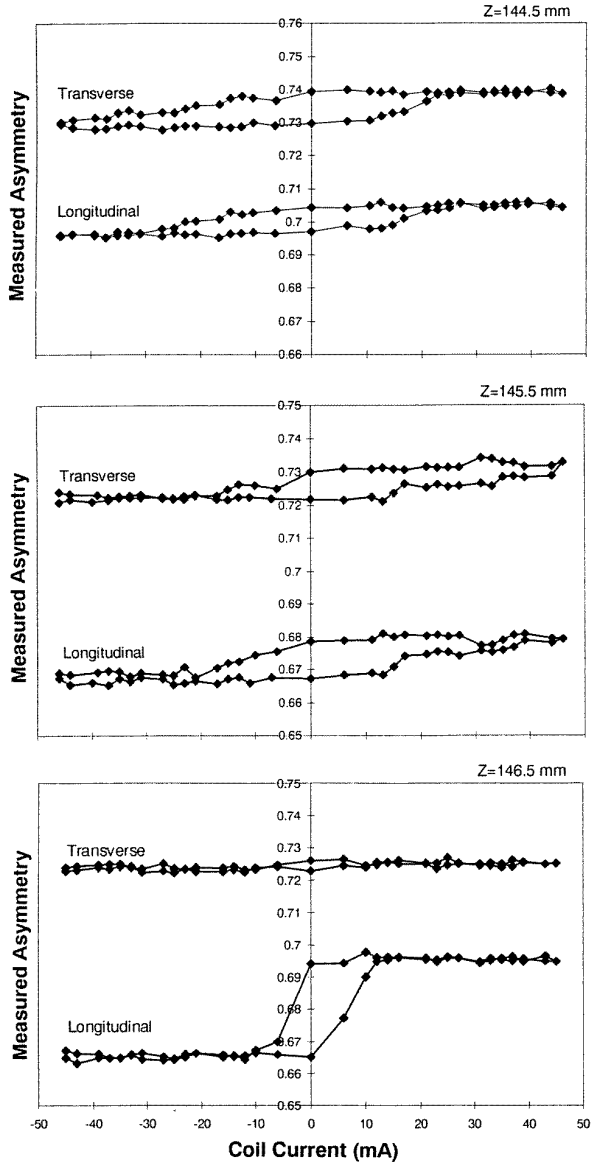

Figure 1. Transverse and longitudinal ERHLs at 1 eV for as-cast $Co_{66}Fe_4Ni_1B_{14}Si_{15}$ obtained using 1.6 keV primary electrons. The errors in this and the following figures are comparable in magnitude to the size of the data points.

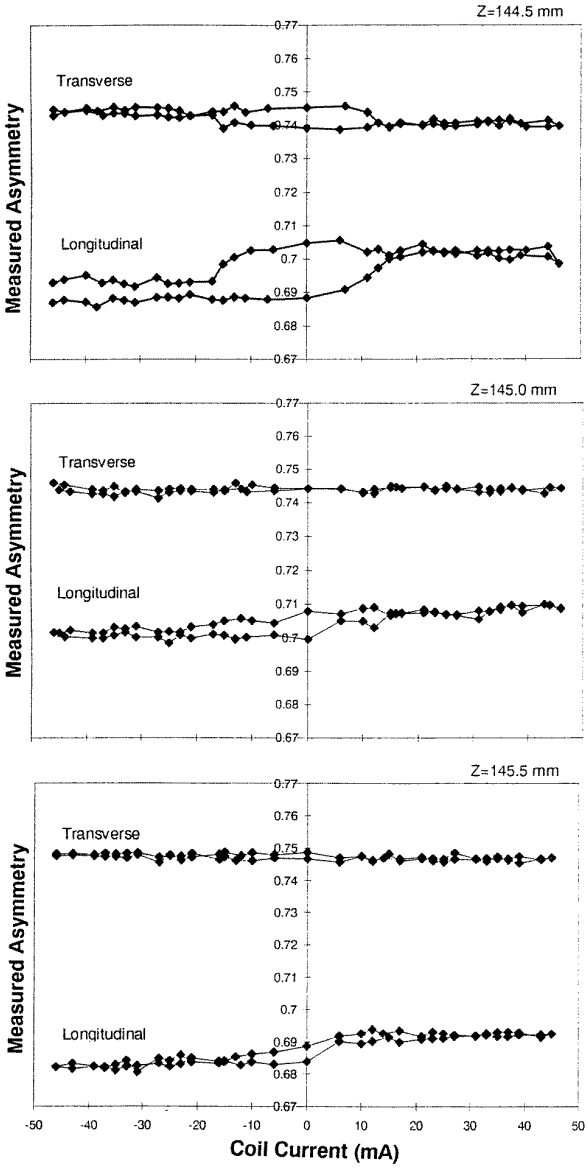

Figure 2. Transverse and longitudinal ERHLs at 0.5 eV for as-cast $Co_{66}Fe_4Ni_1B_{14}Si_{15}$ obtained using 135 eV photons.

behaviour is shown most clearly by the crossing of the two remanent-state asymmetry line scans along XX, which are presented as the upper section of figure 4. It is important to note that the three spot-mode hysteresis loops taken at points along XX, shown as the lower section of figure 4, are rather similar at first sight and thus would not, on their own, immediately suggest that the sample was magnetically inhomogeneous in the remanent state. (A closer examination of the middle loop, taken from the region which is reverse oriented, actually does show clear differences in shape from the other two and the expected time dependence of the lowest current part.)

The top and bottom panels of figure 3 are the SEMPA images taken with the magnetizing current held at its maximum negative and positive values (± 0.5 A, respectively). Labelling these 'saturated' states is clearly incorrect, since the magnetization direction remains fixed over a large proportion of the imaged area, independent of the magnetizing current direction. In particular, the bottom right-hand corners of both these images (and also of the remanent state images) are largely white, so a spot-mode hysteresis loop from most points within this area would not exhibit any significant change in asymmetry with applied current. (Although this region is predominantly blocked in the positive direction, there are some changes occurring on a finer length scale, indicated by the appearance of some reverse-oriented regions in the positive 'saturated'-state image.) It is clear that, despite the very low magnetostriction of this material, there is significant frozen-in anisotropy in its as-cast state which cannot be overcome at 50 times the apparent coercive field.

These SEMPA data are qualitatively similar to those we obtained from as-cast $Fe_{80}B_{20}$ [7], although in that case there was little difference between the remanent- and 'saturated'-state images. Both sets demonstrate graphically

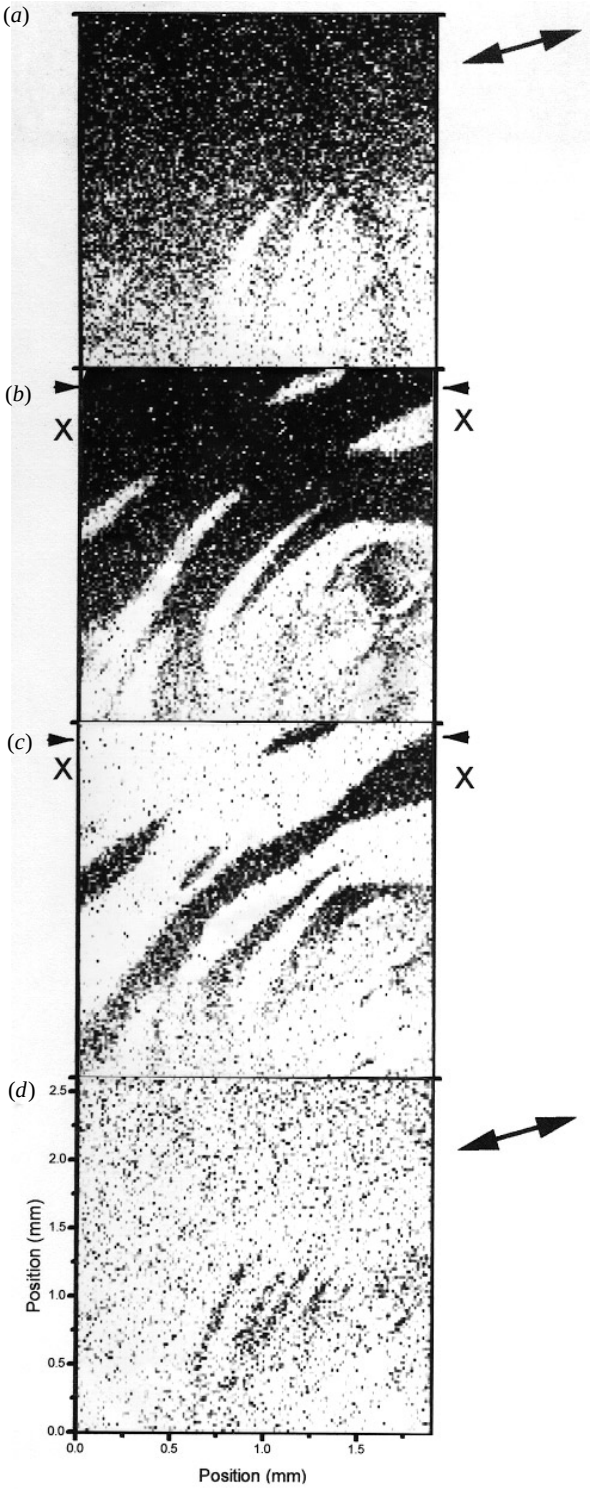

Figure 3. SEMPA images $A_{Long}(x, y)$ from an as-cast sample of $Co_{66}Fe_4Ni_1B_{14}Si_{15}$. Negative (*a*) and positive (*d*) 'saturated' state images, repectively, recorded with the maximum magnetizing current (0.5 A) applied to the sample. Negative (*b*) and positive (*c*) remanent-state images, respectively, taken with zero magnetizing current. The longitudinal (roll) axis is indicated by the double-headed arrow and XX shows the direction of the linescans of figure 4.

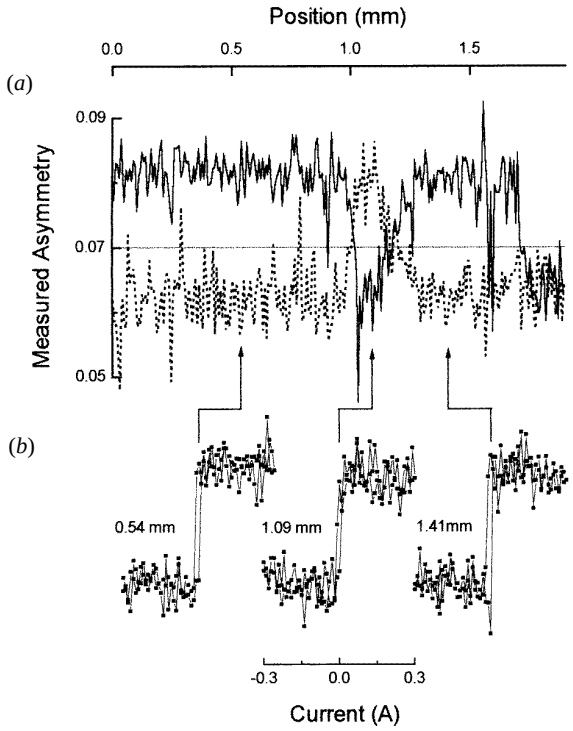

Figure 4. (*a*) Asymmetry line scans $A_{Long}(x)$ along the line XX in figure 3 for the positive (full line) and negative (broken line) remanent states. (*b*) Spot-mode hysteresis loops $A_{Long}(I)$ at three points along the line XX. The vertical scale is common to both sections.

the problems involved in using either the remanent or (apparently) saturated states of as-cast metglas ribbons as polarization standards for electron spectroscopy, particularly when broad-beam techniques are used.

In an attempt to improve the magnetic homogeneity of the sample, field annealing of pre-cut ribbons was carried out to temperatures below the crystallization temperature of the alloy. The field was applied parallel to the long axis of the sample once it had reached the annealing temperature and was removed only when the sample had cooled to below the Curie temperature. Field annealing has been applied to nanocrystalline $Fe_{73}Cu_1Nd_3Si_{13.5}B_9$, for example, and shown to result in squarer hysteresis loops [17]. Figure 5 presents electron-excited ERHLs from the field-annealed material which still reveal large lateral variations in polarization. There is evidence that there has been a slight improvement in homogeneity, leading to squarer loops and slightly higher asymmetry amplitudes over some of the sampled areas. However, there are still areas where the amplitude is very small and the data from areas with large values of A_{Long} also have significant A_{Trans}. This is further demonstrated clearly by the asymmetry spectra $A_{Long,Trans}(E_k)$, given in figure 6, which are very similar to those from as-cast samples. In particular, a large transverse asymmetry is still observed at low secondary electron energies.

We have also investigated the possibility of achieving a reproducible asymmetry by deposition of a thin film of iron onto the surface of unannealed $Co_{66}Fe_4Ni_1B_{14}Si_{15}$. Although this approach lacks the simplicity of a simple ribbon sample as a source of polarized electrons, it is still easier than the use of a single-crystalline sample or a negative-electron-affinity polarized electron source. This experiment also has

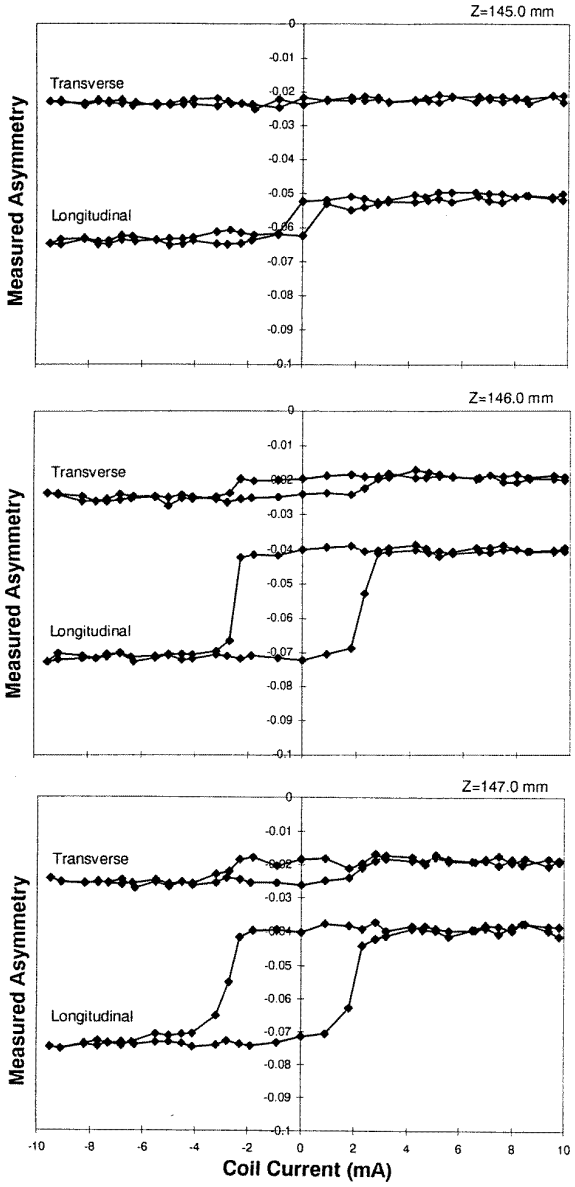

Figure 5. Transverse and longitudinal ERHLs at 1.5 eV for field-annealed $Co_{66}Fe_4Ni_1B_{14}Si_{15}$ obtained using 1.6 keV primary electrons.

some bearing upon the use of alloy ribbons as substrates for the deposition of thin films which are then magnetized by the strong exchange coupling between the substrate and the film. If the domain structure in the substrate persists in the film, then clearly experimentation on the film will result in position-dependent data. We found that low-energy EHRLs, whilst exhibiting, as expected, larger asymmetry changes than those for the uncoated ribbon, again proved to be position dependent. This confirms the findings of VanZandt *et al* [18] that deposition of an iron overlayer onto a ferromagnetic substrate is an effective means of enhancing the polarization of the underlying substrate domain structure.

Overall, the results clearly show that both as-cast and field-annealed samples of $Co_{66}Fe_4Ni_1B_{14}Si_{15}$ are magnetically inhomogeneous. The majority of our SEMPA images from cobalt ribbons contain evidence of domain

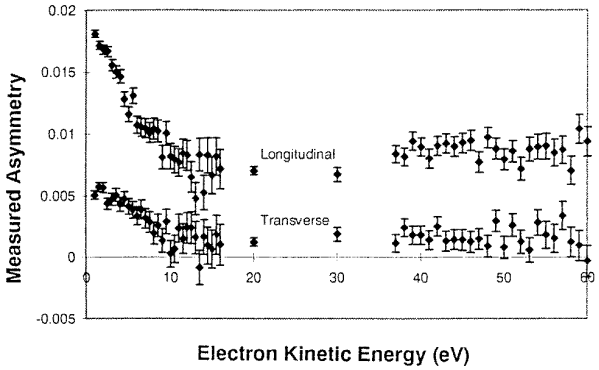

Figure 6. Secondary electron asymmetry spectra $A_{Long,Trans}(E_k)$ of field-annealed $Co_{66}Fe_4Ni_1B_{14}Si_{15}$ obtained using 1.6 keV primary electrons.

structure due to locked-in anisotropy. The lateral scale of these structures is larger and they are less complicated than those found in the high-concentration iron metglasses, but in both cases they have clear correlations to the roll direction and they change after annealing. In the light of Flanders and Morito's observation [19] of creep-induced anisotropy in $Co_{66}Fe_4Mo_2Si_{16}B_{12}$, a material which exhibits zero (bulk) magnetostriction, we therefore attribute the locked-in anisotropy we observe at the surface of $Co_{66}Fe_4Ni_1B_{14}Si_{15}$ to residual strains resulting both from the melt-spinning fabrication process itself and from forming the material into a closed loop (which is necessary in order to minimize stray magnetic fields). We are at present unable to ascertain to what extent such anisotropy persists away from the surface.

4. Summary

The secondary electron polarizations of $Co_{66}Fe_4Ni_1B_{14}Si_{15}$, in particular, and melt-spun amorphous ribbons, in general, are strongly position dependent, indicating that they are not suitable as standard sources of polarized electrons. Deposition of iron onto the ribbons does not result in a more magnetically uniform surface–rather it serves to emphasize the substrate magnetic structure–thus utilization of ferromagnetic melt-spun amorphous alloys as substrates for the growth of thin magnetic films should only be undertaken with caution.

Acknowledgments

The authors would like to thank the EPSRC for studentships (to AERM and SC) and for financial support of this work, the ORS and the University of Leeds for support (to YBX) and Allied Signal Inc for the provision of samples. We also wish to thank L Klebanoff for providing a sample of $Co_{66}Fe_4Ni_1B_{14}Si_{15}$, for helpful discussions and for making data available prior to publication.

References

[1] Kirschner J and Koike K 1992 *Surf. Sci.* **273** 147
[2] Hopster H 1987 *Phys. Rev. Lett.* **36** 2325
[3] Hembree G G, Unguris J, Celotta R J and Pierce D T 1987 *Scanning Microsc. Suppl.* **1** 229

[4] Heyderman L J, Chapman J N, Gibbs M R J and Shearwood C 1995 *J. Magn. Magn. Mater.* **148** 433
[5] Tittes W, Santos A D, Reininger T and Kronmuller H 1992 *Phys. Status Solidi* a **133** 465
[6] Koike K, Matsuyama H, Tseng W J and Li J C M 1993 *Appl. Phys. Lett.* **62** 2581
[7] Seddon E A, Xu Y B, Greig D, Wardell I R M, Rubio-Temprano D and Hardiman M 1997 *J. Appl. Phys.* **81** 4063
[8] Livingston J D, Morris W G and Luborsky F E 1982 *J. Appl. Phys.* **53** 7837
[9] Squire P T, Thomas A P, Gibbs M R J and Kuzminski M 1992 *J. Magn. Magn. Mater.* **104–107** 109
[10] Currie R A 1994 *Ferromagnetic Materials Structure and Properties* (London: Academic)
[11] Klebanoff L E, Van Campen D G and Pouliot R J 1993 *Rev. Sci. Instrum.* **64** 2863
[12] Klebanoff L E, Van Campen D G and Pouliot R J 1994 *Phys. Rev.* B **49** 2047
[13] Sirotti F, Bosshard R, Prieto P, Panaccione G, Floreano L, Jucha A, Bellier J D and Rossi G 1998 *J. Appl. Phys.* **83** 1563
[14] Xu Y B, Walker C G H, Greig D, Seddon E A, Kirkman I W, Quinn F M and Matthew J A D 1996 *J. Phys.: Condens. Matter* **8** 1567
[15] Hardiman M *et al* 1995 *Polarised Electron Polarized Photon Physics* ed H Kleinpoppen and W R Newell (New York: Plenum) p 147
[16] Furakawa T and Koike K 1996 *Surf. Sci.* **347** 193
[17] Herzer G 1993 *Phys. Scr.* T **49** 307
[18] VanZandt T, Browning R and Landolt M 1991 *J. Appl. Phys.* **69** 1564
[19] Flanders P J and Morito N 1984 *J. Appl. Phys.* **55** 1778